2002

Effect of 6-Thioguanine and Methyl-6-Thioguanine on stability of DNA duplexes

Mabaera Rodwell
Colby College

Follow this and additional works at: https://digitalcommons.colby.edu/honorstheses

Part of the Chemistry Commons

Recommended Citation

Effect of 6-Thioguanine and Methyl-6-Thioguanine on Stability of DNA Duplexes

By Mabaera Rodwell

Department of Chemistry, Colby College, Waterville, ME 04901

Effect of 6-Thioguanine and Methyl-6-Thioguanine on Stability of DNA Duplexes

By Mabaera Rodwell

Presented to The Department of Chemistry,
Colby College, Waterville, ME
In Partial Fulfillment of the Requirements for Graduation
With Honors in Chemistry

Stephen U. Dunham
Advisor, Assistant Professor of Chemistry

Shari U. Dunham
Assistant Professor of Chemistry

Department of Chemistry
Colby College
Waterville, ME 04901
May 2002

Dedicated to the country and people of The Republic of Zimbabwe

Abstract:

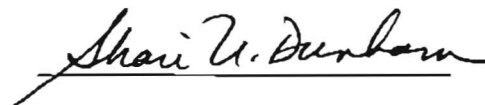6-Thioguanine (^{6S}G) has been used for the past thirty years as an anti-cancer agent in maintenance chemotherapy for childhood acute lymphoblastic leukemia as well as acute myeloid leukemia. Despite its long-standing clinical use, little is understood of the molecular basis of the cytotoxicity associated with ^{6S}G. Research has shown that ^{6S}G is incorporated into DNA during replication after which it may exert its cytotoxicity by inducing rapid mutation or by affecting DNA-protein interactions. ^{6S}G has also been shown to impair HIV replication by inhibiting HIV-1 reverse transcriptase and to inhibit human telomerase activity. To further understand the structural changes associated with DNA duplexes containing ^{6S}G and its metabolite methyl-6-thioguanine (^{Me6S}G), we have studied and compared the thermodynamic properties of the 11 base pair duplex d(CGTTAGATGCC)•(GGCATCTAAGC) to duplexes in which the central G residue is replaced by either ^{6S}G or ^{Me6S}G using temperature dependent UV-Vis experiments. Results suggest that duplexes with ^{6S}G are very similar in stability to those containing normal G while the duplexes with ^{Me6S}G are considerably destabilized compared to G or ^{6S}G.

Vitae

Rodwell son of Ceceilia and Richard Mabaera of Chinhoyi, Zimbabwe completed high school studies in Zimbabwe before coming to the United States for the first time to attend Colby in 1999. At Colby, he studied Chemistry and Mathematics (and only Chemistry and Mathematics) for three solid years and will be moving on to medical school in the fall of 2002. He was also involved with the Colby Cross-Country Team and was member of the Colby Outdoor Orientation Trips (COOT^2) Committee for two years.

Rodwell started work with Stephen Dunham during summer 2000 and has been working in the background since then. The result of which is this project, 'Effect of 6-thioguanine and methyl-6-thioguanine on stability of DNA duplexes.'

Acknowledgements

I here express my sincere gratitude to Dr Stephen and Shari Dunham who despite other commitments were helpful in every way in making this project a success, and for providing a platform for me to do research. Along with them I also want to thank all the students who laid out the groundwork before me and those who provided great help and company during my hours in lab. In addition I would like to thank the Colby Natural Science Division, The National Science Foundation and Howard Hughes Medical Institute for proving funding at various stages of this project. Special thank you to my family who despite being a few thousand miles away, did not fail to call and encourage me each step of my college career.

Table of Contents

List of Figures

9

List of Tables

Introduction:

^{6S}G is a widely used and a clinically accepted metabolic inhibitor with known antitumor, antineoplastic, and immunosuppressive activity (2, 8, 10, 15) Clinically, virtually all major protocols for treating average or low risk acute lymphoblastic leukemia (ALL) and acute myeloid leukemia (AML) have included a core component of maintenance therapy which prescribes daily doses of ^{6S}G or 6-mercaptopurine (6MP), an analogue of ^{6S}G that is metabolized in the same way (2). Along with several other DNA base analogues (Fig 1), ^{6S}G was discovered in 1951 by Gertrude B. Elion and due to the evidence that 6MP and ^{6S}G could produce complete remission in children with ALL, the drug was approved by the Food and Drug Administration barely two years after its first synthesis (8).
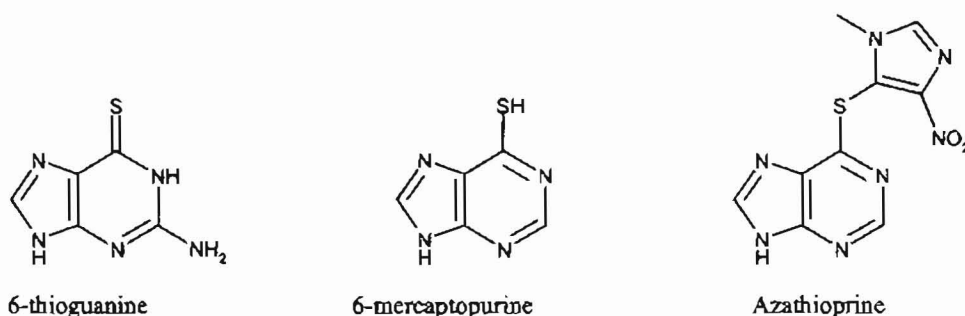
Figure1: Some of the DNA base analogues developed by Elion

In addition, the related prodrugs azathioprine (AZA) and 6MP have also been used as immunosuppressants in preventing rejection of transplanted tissue as well as in the treatment of inflammatory bowel disease (7, 15) and psoriasis (18).

Despite its use for over three decades, the mechanism by which ^{6S}G exerts its cytotoxicity is not fully understood. To date it is known that incorporation of ^{6S}G into DNA of replicating cells is essential for its activity as an antimetabolite and metabolism

of AZA and 6MP has been shown to be mediated through their conversion to 6-thioguanosine triphosphate ([6S]GTP) and subsequent incorporation into DNA by the action of DNA polymerase (Fig. 2) (12).
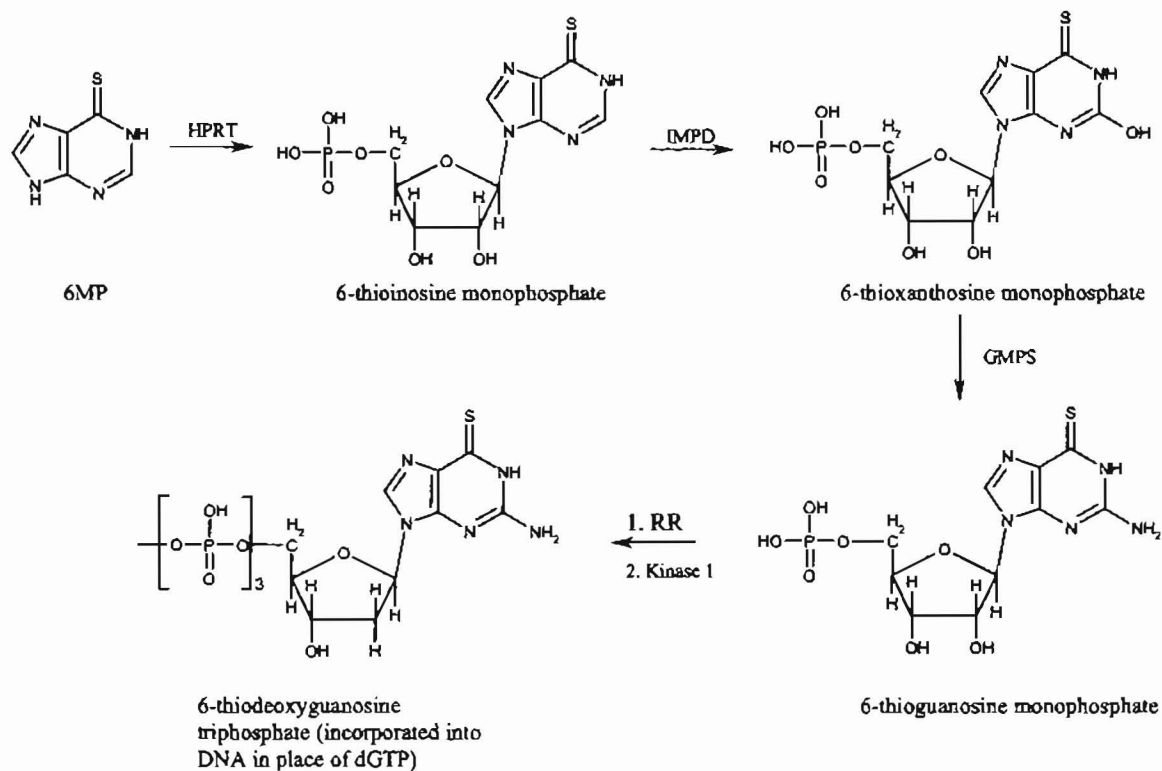
Figure 2: Pathway for the metabolism of 6MP to [6S]G. HPRT, hypoxanthine phosphoribosyltransferase; IMPD, inosine monophosphate dehydrogenase; GMPS, guanosine monophosphate synthetase; RR, ribonucleotide reductase; Kinase 1, phosphoribosylpyrophosphorylase.

Upon incorporation into DNA initial suggestions are that the larger Van der Waals radius and reduced electronegativity of sulfur, (and hence longer C=S bond) considerably weaken the normal Watson-Crick hydrogen bond interaction between [6S]G and C leading to distortion of the DNA helical structure (4). And similar to guanine, a number of different tautomeric forms are possible. Infrared experiments carried out at 12 K (10) as well as theoretical calculations (21) have shown that the amino-thiol (N9H, Fig. 3-1)

12

is the most stable tautomer of isolated ^{6S}G in hydrophobic environments and it was

shown to exist in almost equal equilibrium with another amino-thiol (N7H, Fig. 3-2).

1   2
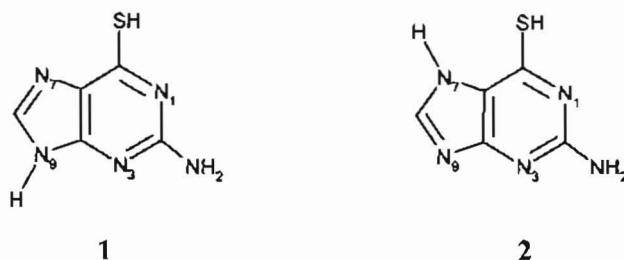
Figure 3: Most stable tautomers of isolated ^{6S}G by experiment in hydrophobic
environment at 12 K. Also obtained by calculation.

This observation may support other evidence that ^{6S}G in duplex DNA may encode

equally for C or T during replication (12) as amino-thiol tautomers allow for a more

stable three hydrogen bond interaction with T (Fig. 4).

1   2
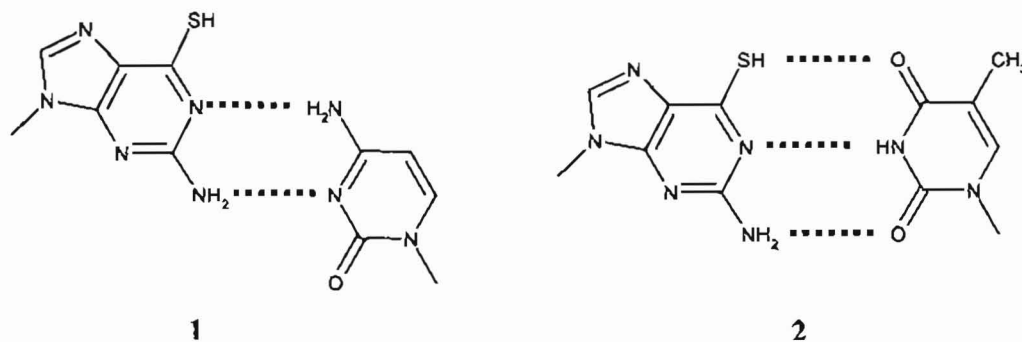
Figure 4: Base pairing of amino-thiol tautomer with C (1) and T (2).

This ^{6S}G•T mismatch was thought to be a major contributor towards the DNA damage via

recognition of the mismatch DNA repair proteins (11) or through subsequent single base

point mutations after several rounds of DNA replication (Fig. 5).
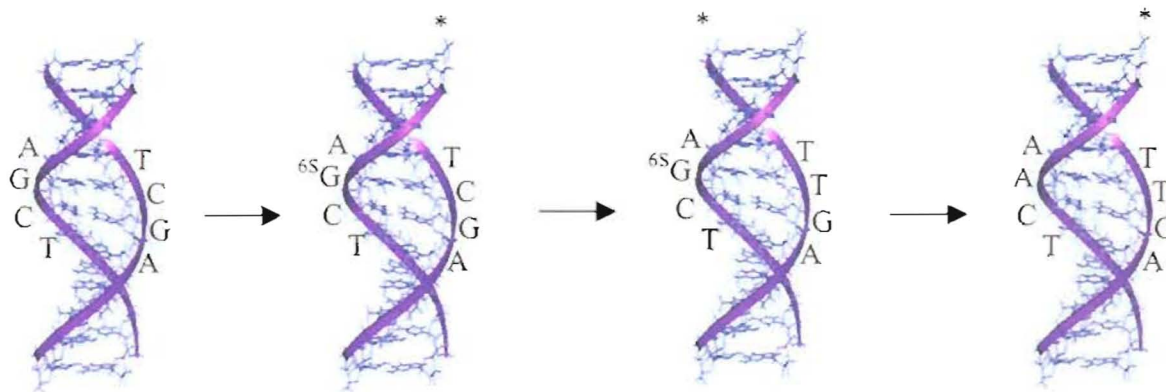
Figure 5: Possible scheme for G to A point mutations due to ^{6S}G•T mismatch (replicated strands are shown with an asterisk).

Another way in which incorporated ^{6S}G may damage duplex DNA is through formation of disulphide bridges which result in DNA-protein cross-links and/ or formation of interstrand cross-links and sister chromatid exchanges during DNA replication (2, 14). In addition, the distortion of the helical structure may lead to alteration of key DNA-protein interactions, which contribute to the cytotoxicity associated with ^{6S}G. Particular examples of protein-^{6S}G interactions include inhibition of HIV-1 reverse transcriptase (11, 24) and human telomerase activity (16). These discoveries may contribute to the development of new antiretroviral agents or shed some light on how antitumor activity is achieved. Closely linked to this is the fact that ^{6S}G is destabilizing enough to prevent the formation of quadruplex structures, which are an important structure in telomeric DNA (13).

Another pathway that is implicated in the mode of action of ^{6S}G involves methylation of the ^{6S}G residue. Incorporated ^{6S}G is converted to the methylated residue by action of S-adenosylmethionine (Fig. 6)

S-adenosylmethionine
(SAM)
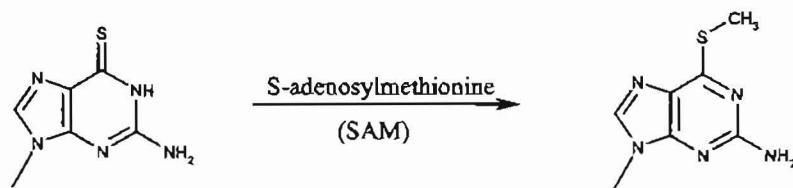
Figure 6: Pathway for the metabolism of ^{6S}G to give ^{Me6S}G

Similar to ^{6S}G, ^{Me6S}G is known to code equally for T and C during replication and is thus generally believed to produce the same effects as ^{6S}G. Recent work has revealed that proteins of the postreplicative repair system recognize and bind to ^{Me6S}G•C base pairs in a sequence specific manner (23). This in turn may suggest that the ^{Me6S}G•C base pair alone changes the structure of duplex DNA enough to lead to mismatch repair errors and the miscoding of T may not be a required step for observed cytotoxicity in the case of ^{Me6S}G.

Thus, the structural changes in the DNA containing ^{6S}G or ^{Me6S}G are important for the interactions that produce the observed clinical effect, and understanding the specific nature of these changes may provide an insight on how ^{6S}G and its prodrugs exert their effect. The goal of this project was thus to obtain a thermodynamic characterization of DNA oligonucleotides that have ^{6S}G and ^{Me6S}G incorporated at a specific site and compare them to corresponding oligonucleotides with G in the same position. The synthesis of oligonucleotides with modified bases at predetermined sites has been described (5, 6). The DNA of choice was obtained by positioning the ^{6S}G in the center of a non-selfcomplementary 11 base pair strand (shown below) to give a single full helical turn, which gives a good initial working model for understanding DNA containing ^{6S}G.

5' d(CGTTAG*ATGCC)   3'

Having a non-selfcomplementary model ensures that only one duplex adduct is formed. Strands were synthesized and duplexes were formed for all the possible pairings of G•C, G•T, ^{6S}G•C, ^{6S}G•T, ^{Me6S}G•C and ^{Me6S}G•T.

Materials and Methods:

General:

Reagents were used as obtained from Fisher Scientific with the following exceptions. Phosphoramidite and DNA synthesis columns were obtained from Glen Research. 1-Amino-2-naphthol-4-sulfonic acid (technical grade), *p*-toluenesulfonic acid, $(NH_4)_6Mo_7O_{24} \cdot 4H_2O$ and $Na_2SO_3 \cdot 7H_2O$ were obtained from Eastman Organic Chemicals. Solutions were made using deionized water from a MilliQ purifier.

Synthesis of Oligonucleotides:

Synthesis of oligonucleotides was carried out on a 1.0 or 2.5 μmole scale using an Applied Biosystems PCR-MATE 391 DNA synthesizer. The synthesis of DNA sequences with modified bases at predetermined sites has been well documented (5,6) and 6-thioguanosine phosphoramidite was purchased from Glen Research. Strands synthesized by phosphoramidite methods are shown below.

5' d(CGTTAGATGCC) 3'	**1**
5' d(CGTTA^{6S}GATGCC) 3'	**2**
5' d(GGCATCTAACG) 3'	**3**
5' d(GGCATTTAACG) 3'	**4**

Oligonucleotides were cleaved from the column by incubation with conc. NH₄OH (50 mM NaHS in conc. NH₄OH for oligonucleotides containing ^{6S}G) at 25°C for 10 min (quick-deprotect column) or 30-45 min (standard column). Complete deprotection of all

functional groups was achieved by further incubation at 55°C for 4–6 hr (or at 25°C for 12-16hr). Methylation of ^{6S}G was done using methyl iodide (85μM DNA, 6 eq. of CH$_3$I, 6 hr, 25 °C, unbuffered) to obtain **5** from **4**.

$$5' \quad d(CGTTA^{Me6S}GATGCC) \quad 3' \qquad \textbf{5}$$

Overall yields for DNA syntheses were 83-88% as determined by UV-Vis analysis of trityl cations at 595 nm. Yields for **2** were lower compared to DNA without ^{6S}G due to the lower coupling efficiency of the ^{6S}G phosphoramidite. Duplex formation was done by mixing estimated molar equivalents of the appropriate strands at room temperature.

Purification:

Initial purification of single strands was done using a Sephadex G-25 gel filtration column (100 mm x 18 mm) by eluting 1 mL of DNA solution with H$_2$O. Fractions from gel filtration were purified using ion exchange high performance liquid chromatography (HPLC) on a Waters Gradient Controller with a Dionex Chromatography DNAPac PA-100 column (9 mm x 250 mm, quaternary amine functionality on non-porous resin support), NaCl gradient (Tables 1a and b) in 10% ACN, 0.025 M NH$_4$OAc pH 6.8, flow rate 5.0 mL/min and monitored by UV detector at 260nm.

Table 1: Gradient for Purification of single strands.

a.

Time / min	%A	%B
0	100	0
30	60	40
35	0	100

18

b.

Time / min	%A	%B
0	75	25
20	50	50
30	0	100

c.

Time / min	%A	%B
0	100	0
30	50	50
40	0	100

Table 1: (a) Gradient used to purify non-methylated strands, (b) gradient for methylated strand, (c) gradient for purification of duplex DNA. Buffer A: 0.025 M NH$_4$OAc (pH 6.8) in 10% ACN Buffer B: 1.0 M NaCl, 0.025 M NH$_4$OAc (pH 6.8) in 10% ACN

Since the desired 11mer was the longest fragment, it eluted last off the column (21-23 min) and thus collection was easy and purification was done with virtually no further loss of the product. Fractions from ion exchange HPLC were then lyophilized followed by resuspension in water and final desalting of the DNA samples by gel filtration (Sephadex G-25 column, 100 mm x 18 mm, 1 mL DNA solution). DNA samples were lyophilized and resuspended in a final volume of 500 μL water (15 mM DTT solution for strands with [6S]G) for storage. Samples containing [6S]G or [Me6S]G were stored in 10 mM Dithiothreitol (DTT) to prevent oxidative loss of sulfur.

Qualitative Analysis of SS DNA:

Purity of the synthesized oligonucleotides was estimated by running analytical HPLC on a Dionex Chromatography DNAPac PA-100 column (4 mm x 250 mm). Gradients identical to those used for purification were employed with the flow rate

19

reduced to 1.0 mL/min. Samples were estimated to be 90-98% pure (disregarding the lower extinction coefficients for the shorter fragments).

Stability of strand **5** containing ^{Me6S}G was monitored over time and in different environments by taking ~5 nmole amounts and analyzing them by HPLC at 24 hr intervals. Conditions investigated were: (a) stability in water solution at 25 °C, (b) stability in 10 mM DTT solution at 25 °C and (c) stability after heating and cooling cycle (25-70 °C over ~20 min). Strand **5** was also characterized by mass spectrometry on an Agilent Quadrapole Ion Trap SL (infusion mode, electrospray ionization, negative ion mode, scan range 200.00 m/z to 2200.00 m/z, 5 spectra averages).

Quantitation of Duplex DNA:

Duplex DNA for van't Hoff analysis was quantitated by molybdate phosphate analysis using a modification of the method developed by Griswold et al (9). DNA duplex, about 2 nmole was hydrolyzed by incubating in 36 N H_2SO_4, (150 μL acid and total volume made up to 300 μL with H_2O) at 200°C for 15 min. After cooling to room temperature, 0.5 mL of 2.5% molybdate solution was added followed by 1.0 mL of 1-amino-2-naphthol-4-sulfonic acid solution (4.5 mM acid, 15.9 mM Na_2SO_3, 0.59 M $NaHSO_3$) and volume was made up 5.0 mL with H_2O. The mixture was heated at 100°C in a water bath for 10 min and after cooling to room temp, volume was readjusted to 5.0 mL then absorbance measured at 820 nm. Absorbance was compared to a standard curve generated using KH_2PO_4 standard solutions, which were given the same treatment as the DNA samples.

Temperature-dependent UV-Vis Experiments:

Duplex melting profiles were obtained in phosphate buffer (10 mM PO_4^{3-}, 100 mM NaCl, 1 mM EDTA, pH = 6.8-7.2) in quartz cells (1.0 cm path length, 600 μL total volume) on an Ocean Optics S2000 UV-Vis spectrophotometer coupled to a Neslab water bath in a custom- made apparatus (Fig. 6).
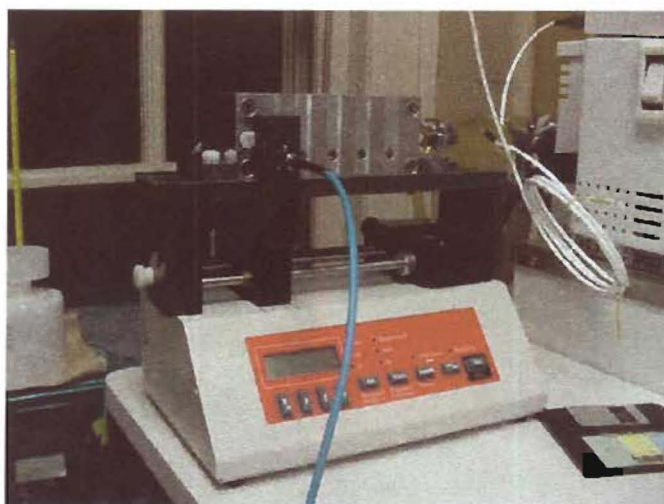
Figure 7: DNA melting apparatus; aluminum 5-cell holder with Neslab™ water bath for temperature control and syringe pump to drive the fiber optic between the cells. Instrument interfaced using LabView™

Apparatus was designed to ensure that all the profiles are obtained under the same conditions with one cell containing a buffer blank to correct for the background absorbance. Temperature was varied in the range 5 °C - 55 °C in 1 °C steps for strands containing ^{Me6S}G, and 15 °C – 65 °C for all the others with a 60 s equilibration time at each temperature. DNA duplex concentration ranged from 3 μM to 30 μM.

Results and Discussion

DNA oligonucleotides containing ^{6S}G and ^{Me6S}G were synthesized by phosphoramidite methods as previously described (5, 9). Purification was done using ion exchange HPLC and duplexes were made by mixing appropriate single strand solutions. To compare the thermodynamic properties of DNA containing the modified base to that with normal G residue, identical duplex sequences differing only in the central base pair were used in temperature-dependent UV-Vis study to determine melting temperatures as well as van't Hoff thermodynamic parameters. Results indicate that DNA oligonucleotides were successfully synthesized and were stable under the conditions used for the thermodynamic studies.

Purification of DNA oligonucleotides

The analytical HPLC trace for DNA single strands before purification in shown in Fig. 8 for strands **1** and **2**. Traces show that the syntheses were relatively efficient at each coupling step as very little of the shorter strands is observed in the two traces shown. Traces for the purification of single strand are shown in Fig. 9 and the DNA fraction collected for analysis is indicated (circled). The purification trace for strand **2** shows that there is a significant amount of 5-mer in the crude DNA indicating the fact that coupling of the ^{6S}G phosphoramidite is not as efficient compared to unmodified bases. Also a peak is observed at 33 min, indicating the presence of disulphide bridged DNA strands. Addition of 15 mM DTT to the DNA solutions reduces the disulphide bridges leading to the absence of 33 min peak in HPLC trace. Similar, but smaller peaks are observed in the other HPLC traces but these may be due to weak interactions between two identical (non-complementary strands.
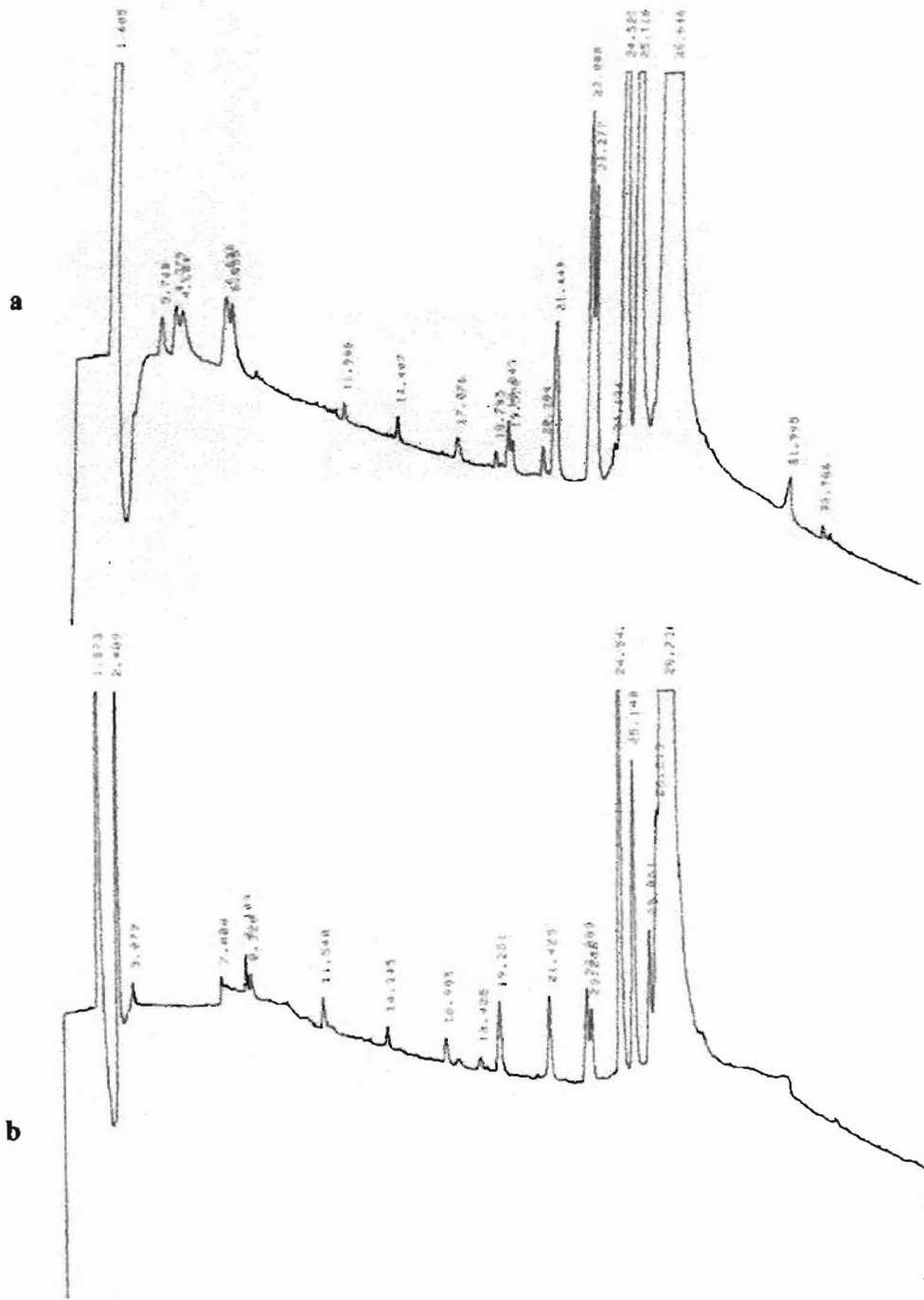
Figure 8: Analytical ion exchange HPLC traces of absorbance (260nm) vs. time (min) for unpurified oligonucleotide single strands. (a) strand 1 and (b) strand 3. Both traces were obtained using linear gradient of NaCl (Table 1a)
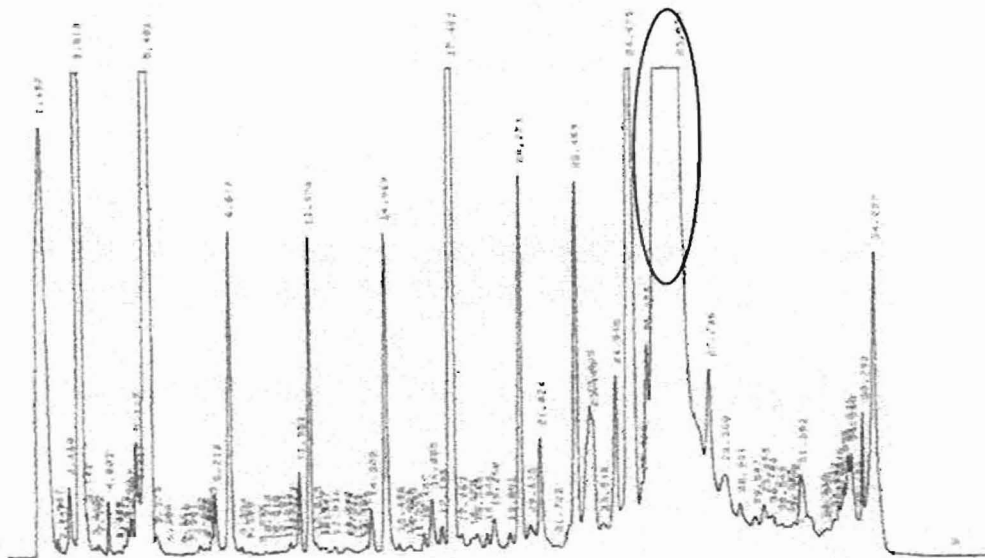
5 Bases long, i.e. no
⁶ˢG coupling

S-S bridge-linked
DNA

Figure 9: Purification of single strands by ion exchange HPLC. Absorbance (260nm) vs.
time (min) for (a) strand **1** and (b) strand **2**. Both traces were obtained using linear
gradient of NaCl (Table 1a)

24

c

d

Figure 9: Purification of single strands by ion exchange HPLC. Absorbance (260nm) vs. time (min) for (c) strand **3** and (d) strand **4**. Both traces were obtained using linear gradient of NaCl (Table 1a)

Analytical traces for the purified single strands are shown below (Fig. 10). Traces indicate the purification was quite efficient and the oligonucleotides obtained had greater than 90% pure single strands.

Figure 10: Analytical HPLC traces of purified oligonucleotides. Absorbance (260nm) vs. time (min) for (a) strand **1** and (b) strand **2**. Both traces were obtained using linear gradient of NaCl (Table 1a)

Figure 10: Analytical HPLC traces of purified oligonucleotides. Absorbance (260nm) vs. time (min) for (c) strand **3** and (d) strand **4**. Both traces were obtained using linear gradient of NaCl (Table 1a)

Synthesis of oligonucleotide with ^{Me6S}G

Synthesis of strand **5** was done by methylating the central ^{6S}G residue in **2** using CH$_3$I in water solution at room temperature to prevent methylation of the O in G residues. Initial experimental conditions were obtained from previous syntheses of ^{Me6S}G (19).

Optimization of the experimental conditions was done by varying concentration of CH_3I as well as the time of reaction (Fig. 11).
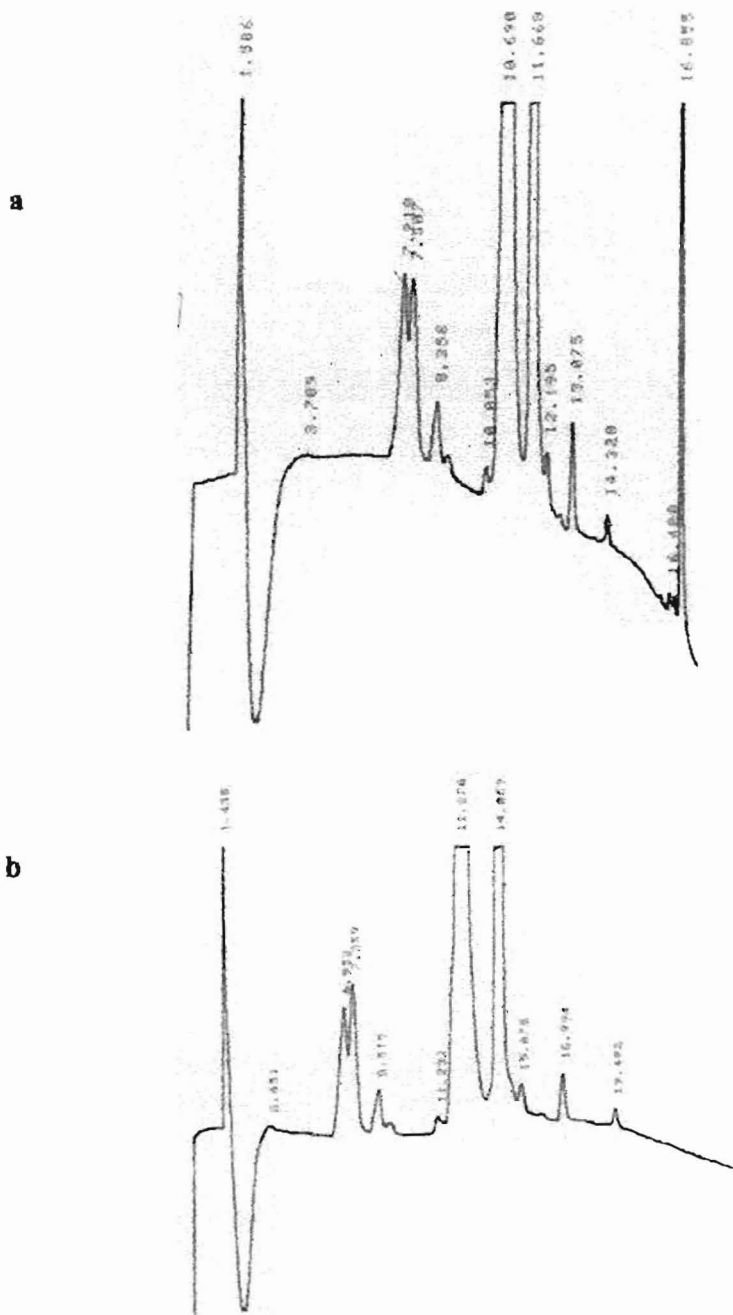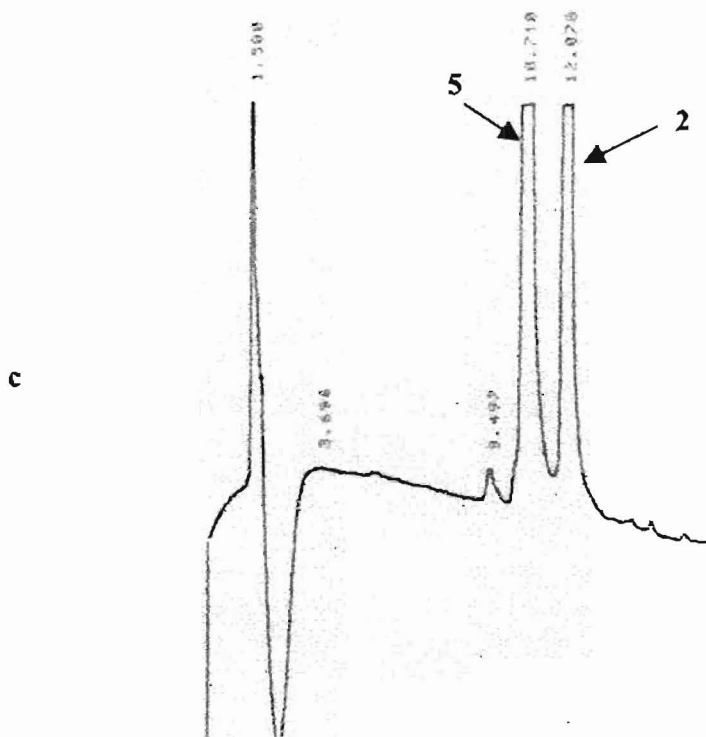
Figure 11: Methylation experiment of ~2 nmole DNA at 85 μM with different concentration of CH$_3$I. (a) 85 mM, (b) 850 μM, and (c) 450 μM. Reactions were carried out at 25°C in unbuffered water solution. Traces were obtained at ~10 min after reaction start.

Results indicate that methylation depends on the concentration of the methylating agent CH$_3$I. At low concentrations (~5 eq. Fig. 11c) two main peaks are observed corresponding to 5 in which only the S6 position on ^{6S}G is methylated. At higher concentrations however (10 and 100 eq., Fig. 11a and b), more peaks are observed suggesting that methylation may be less selective at higher CH$_3$I concentration or that DNA may be undergoing other complicated reactions with CH$_3$I. Thus reactions were done using 6 equivalents of CH$_3$I to optimize both yield and rate of methylation.

The methylation reaction was monitored over time to determine the optimal amount of time for obtaining maximum methylation without promoting methylation of the O6 position in G residues (Fig. 12).
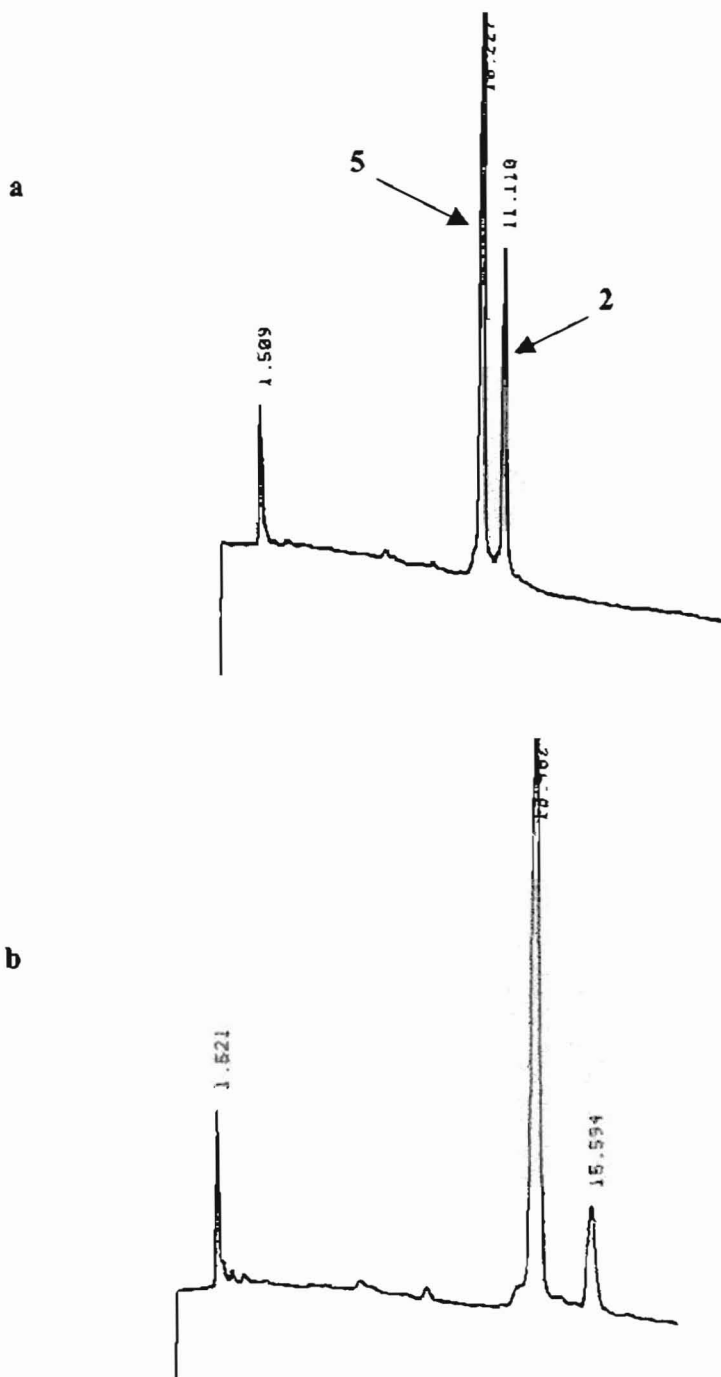
Figure 12: Analytical HPLC traces for optimizing the reaction time for methylation of ^{6S}G by CH_3I, 25 °C unbuffered water solution. (a) reaction (Fig 11c) after 4 hr, NaCl gradient Table 1b and (b) reaction after 7 hr, NaCl gradient 70:30 to 55:45 in 20 min.

Oligonucleotide 5 was then purified (Fig. 13a) and an analytical trace of the purified

oligonucleotide shows that it is more than 95% pure single strand (Fig. 13b).
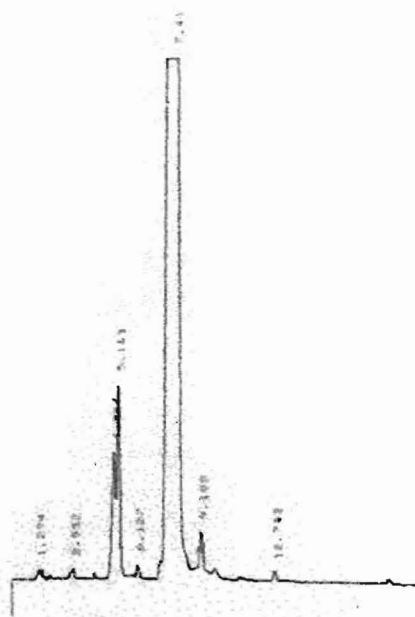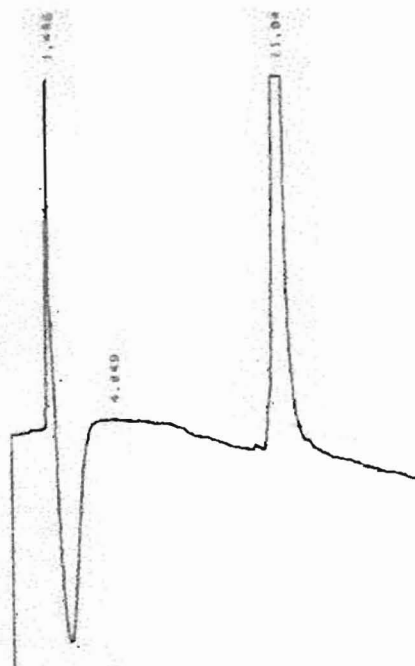
Figure 13: (a) purification of 5 by ion exchange with NaCl gradient (Table 1b) and (b) analytical HPLC trace of the purified DNA.

Stability of strand containing ^{Me6S}G residue

Earlier studies have shown that both ^{6S}G and ^{Me6S}G can undergo oxidative loss of sulfur when incorporated in DNA oligonucleotides (6). Storage of **2** with 10 mM DTT

has been used by Stephen Dunham before for stabilization of the ^{6S}G residue, but no previous long-term storage of 5 had been done. Stability of 5 was monitored over time as well as under different storage conditions. Fig. 14 shows DNA stability when stored in water solution at room temperature. A lower charge fragment appears in small quantities at days three but by day 10, several fragments were observed indicating that the strand undergoes some degradation, possibly oxidative loss of sulfur. Fig. 15 shows stability when 5 was stored in a reducing solution of 15 mM DTT. Virtually no degradation is apparent at day 10. Fig. 16 shows stability after heating in unbuffered water solution (20°C to 60 °C). Significant degradation is observed and this may be due to both oxidation of the S6 position and thermal decomposition. Heating and cooling of duplex DNA in phosphate buffer with 10 mM DTT (used in melting experiments) produced no apparent degradation of the DNA (data not shown).
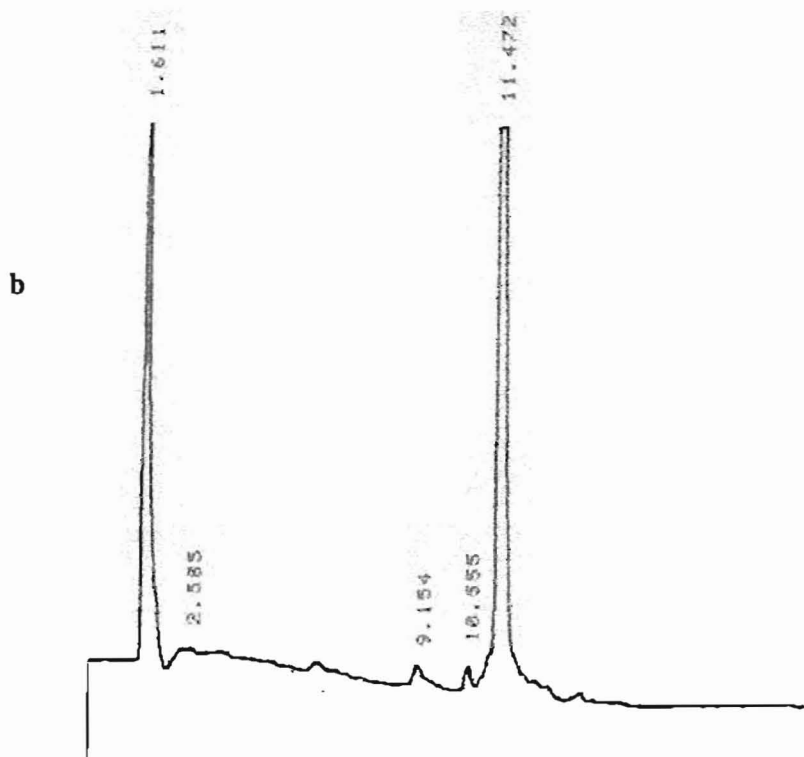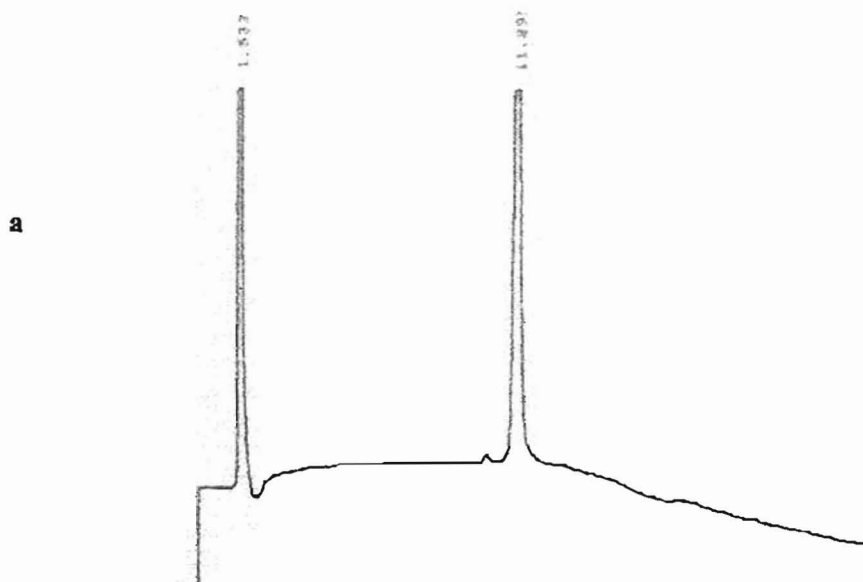
Figure 14: Stability of 5 stored in water solution at (a) 3 days and (b) 10 days of storage at room temperature. Ion exchange HPLC traces obtained using NaCl gradient (Table 1b)
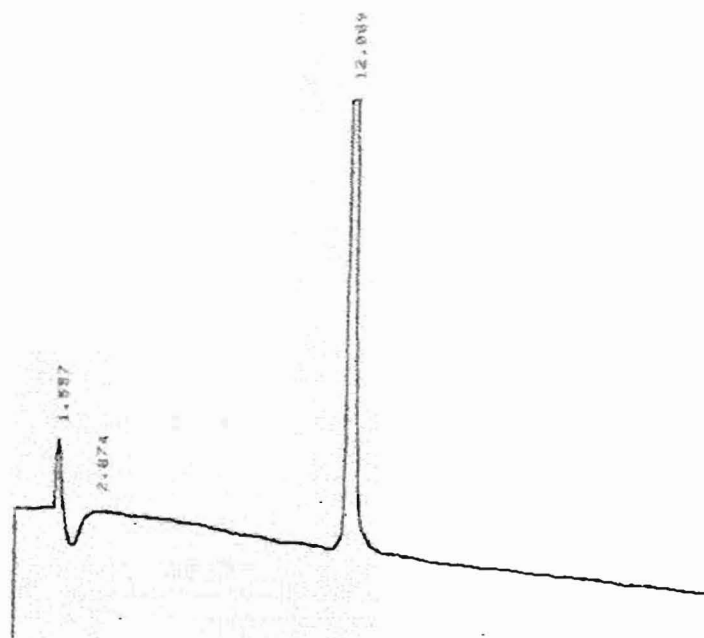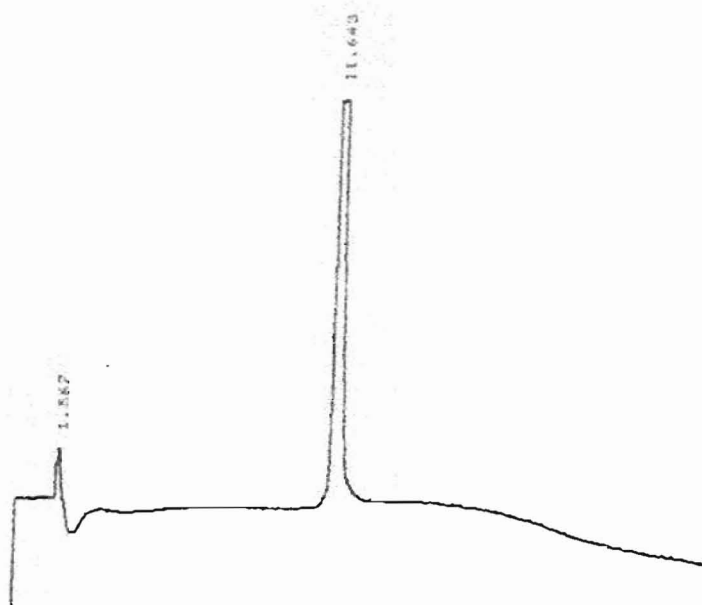
Figure 15: Stability of 5 stored in DTT (15 mM) solution at (a) 3 days and (b) 10 days of storage at room temperature. Ion exchange HPLC traces obtained using NaCl gradient (Table 1b)
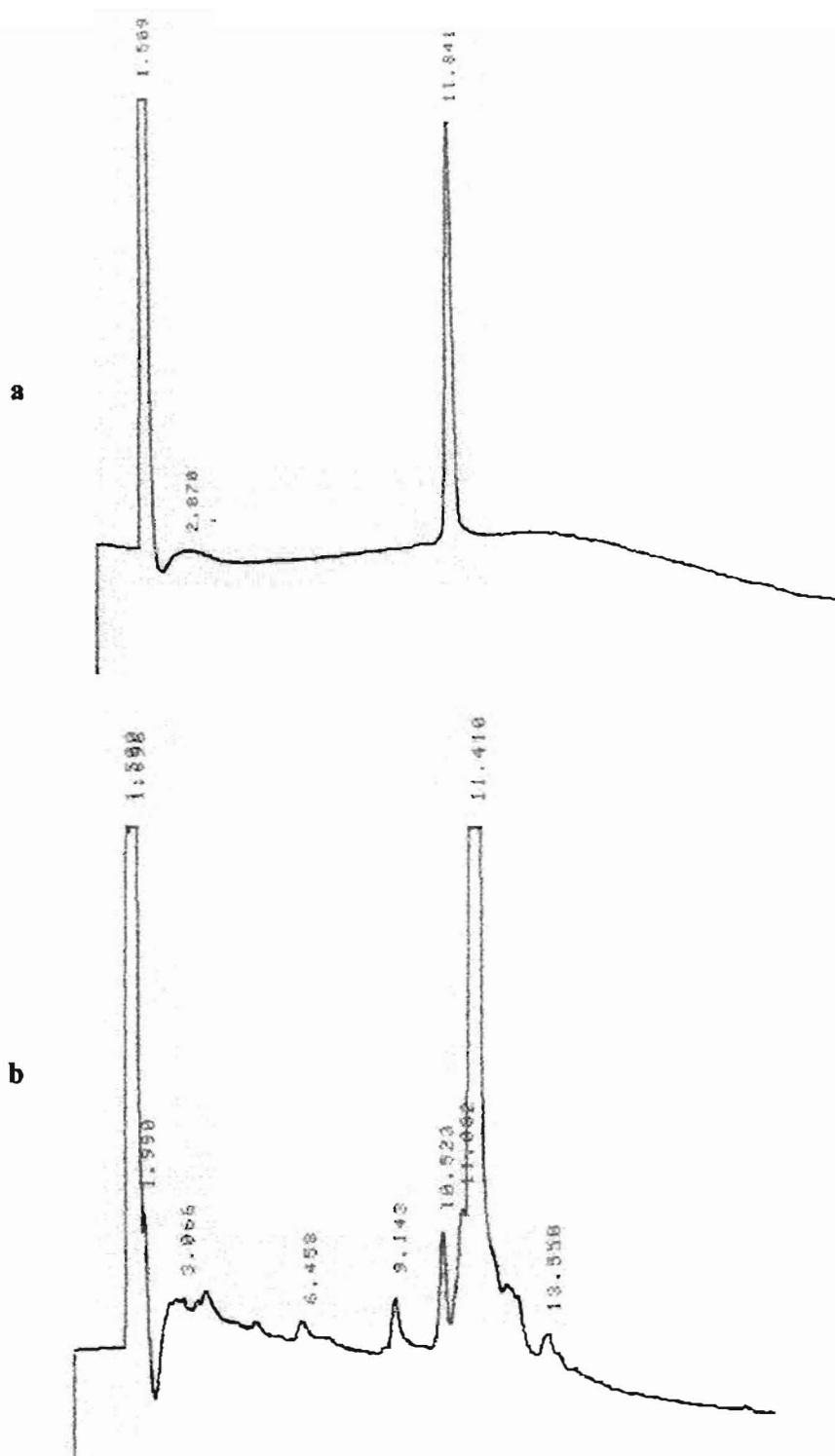
Figure 16: Stability of **5** at elevated temperatures. (a) 25 °C and (b) after heating to 60 °C and cooling to room temperature in unbuffered water solution. Ion exchange HPLC traces obtained using NaCl gradient (Table 1b)

Characterization of strand containing ^{Me6S}G residue

Figure 16 shows the electrospray, negative ion mode mass spectrum of 5 with a base peak at m/z = 1119.3 (calculated value for M^{3-} = 1119.8). This confirms the identity of the synthesized sequence as resulting from methylation only at the S6 position and not at multiple places.
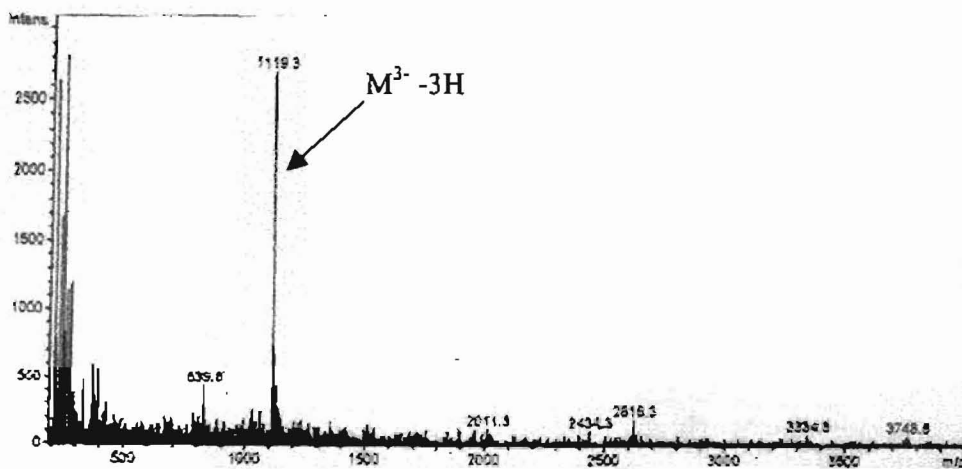
Figure 17: Negative ion mode electrospray mass spectrum of 5.

Duplex formation and purification

The formation of duplex DNA was done by estimating molar equivalents of the appropriate single strands and mixing them at room temperature for five minutes. In some cases duplex reaction mixture was warmed to 60 °C and then allowed to cool slowly to room temperature to speed up the association. Duplex DNA was purified using ion exchange HPLC and analytical traces show over 90% pure DNA (Fig. 18).
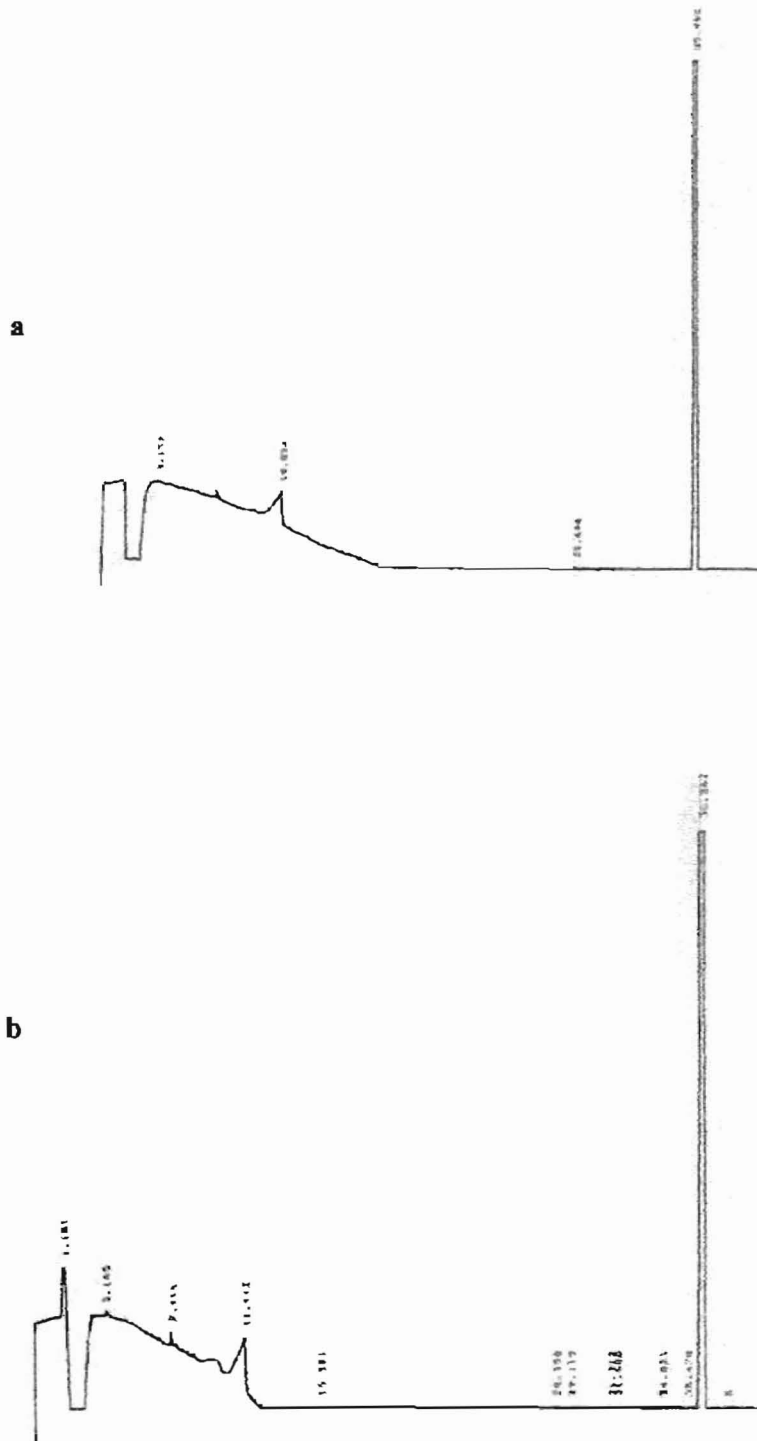
Figure 18: Analytical HPLC traces of purified oligonucleotide Duplexes. (a) 1•3 and (b) 2•3. Both traces were obtained using linear gradient of NaCl (Table 1c)
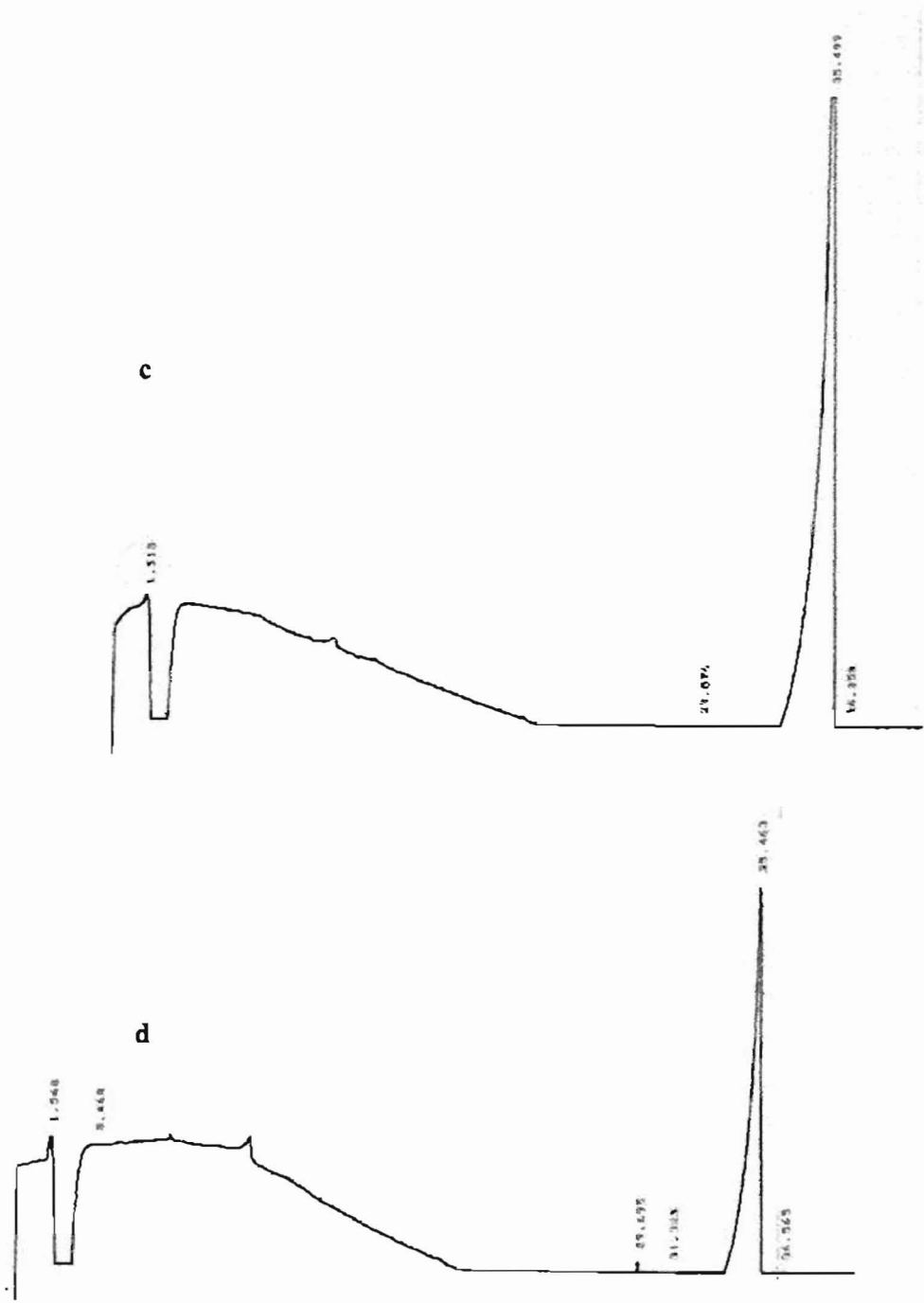
Figure 18: Analytical HPLC traces of purified oligonucleotide duplexes. (c) **1·4** and (d) **2·4**. Both traces were obtained using linear gradient of NaCl (Table 1c)
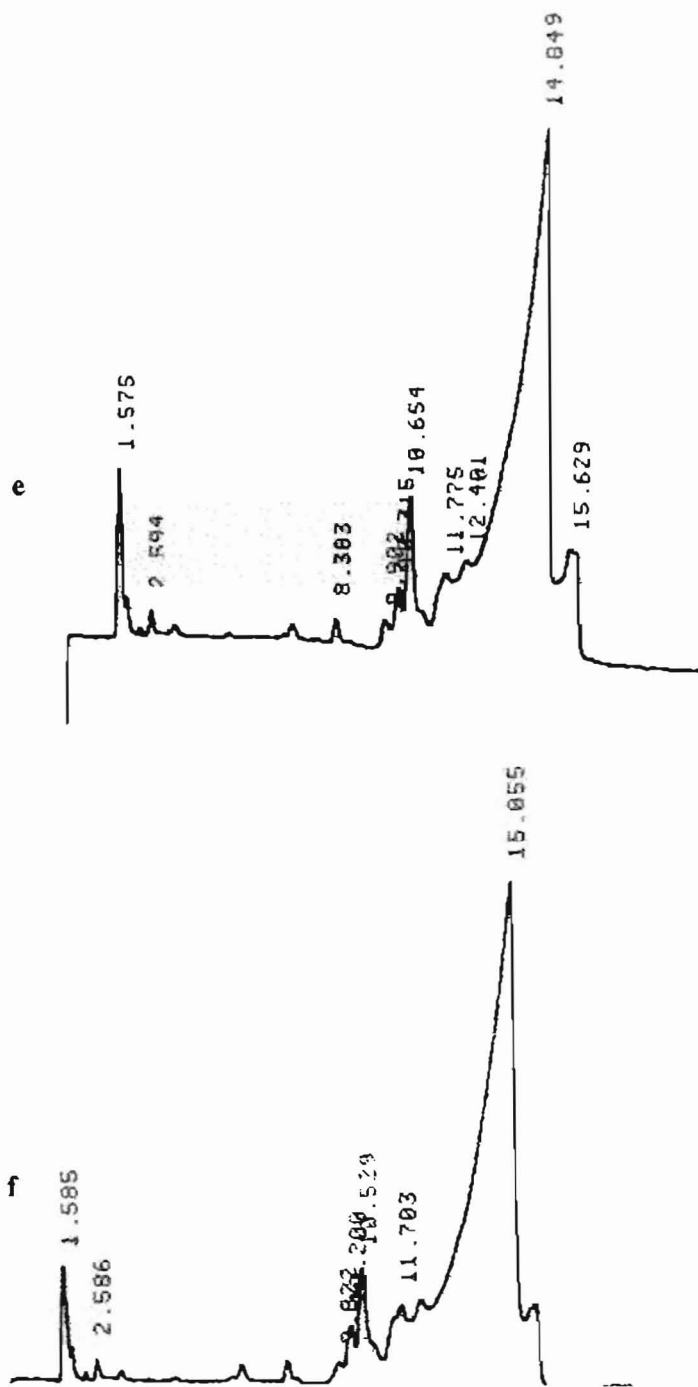
Figure 18: Analytical HPLC traces of purified oligonucleotide duplexes. (e) **5·3** and (f) **5·4**. Both traces were obtained using linear gradient of NaCl (Table 1c)

Determination of duplex DNA concentration:

Concentration of DNA duplexes for van't Hoff analysis was determined by a modification of the method suggested by Griswold et. al. (9). The suggested method uses perchloric acid for digestion of organic samples followed by a quenching of the acid before the phosphate analysis is done in mild acid (9). Instead, concentrated sulfuric acid was used for digestion at microliter quantities and the solution was then diluted to reach the desired volume and concentration of acid for phosphate analysis without quenching of the digesting acid.

The method utilizes the moderately selective reducing solution of 1-amino-2-naphthol-4-sulfonic acid solution (in a $Na_2SO_3/NaHSO_3$ buffer) in the presence of sulfuric acid to promote the formation of a relatively intense blue phosphorous complex of molybdenum, which can be easily monitored by UV-Vis at 820-830 nm. Fig. 19 below shows a typical standard curve for phosphate standards that were treated exactly the same way as DNA samples.

P_i Standard Curve

$y = 0.004710x - 0.01422$
$R^2 = 0.9992$
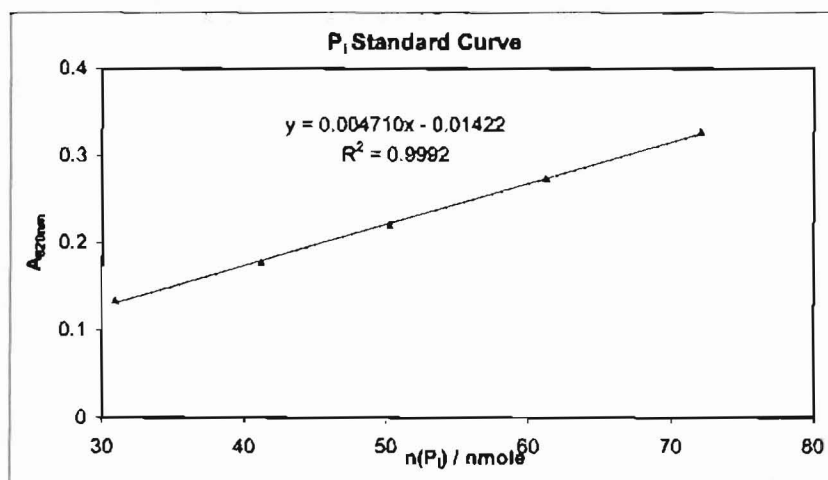
Figure 19: Standard for concentration determination using molybdate phosphate analysis.

Concentrations were determined as an average of two values obtained independently using two different standard curves. Values are reported as means with standard deviation as determined by analysis of standard curve using least squares error analysis as well as variance in the average obtained from the two different standard curves.

Table 4 concentrations of Duplex DNA solutions by phosphate analysis

Duplex	[DNA] / μM	Stdev	%error	ε_{260nm} / $M^{-1}cm^{-1}$
GC	159	11	6.7%	157628
^{6S}GC	157	9	6.0%	132271
^{Me6S}GC	198	17	8.7%	152914
GT	205	13	6.3%	126029
^{6S}GT	96	12	8.3%	185008
^{Me6S}GT	88	15	5.2%	191521

Extracting van't Hoff thermodynamic parameters

The association-dissociation equilibrium for DNA duplexes was monitored using UV-Vis spectroscopy. The resulting curves of absorbance vs. temperature directly depend on the concentrations of duplex vs. single strand at any given temperature. Melting profiles were analyzed using a modification of the method developed by Breslauer et al (3). A typical melting profile is shown in Fig. 20 below.
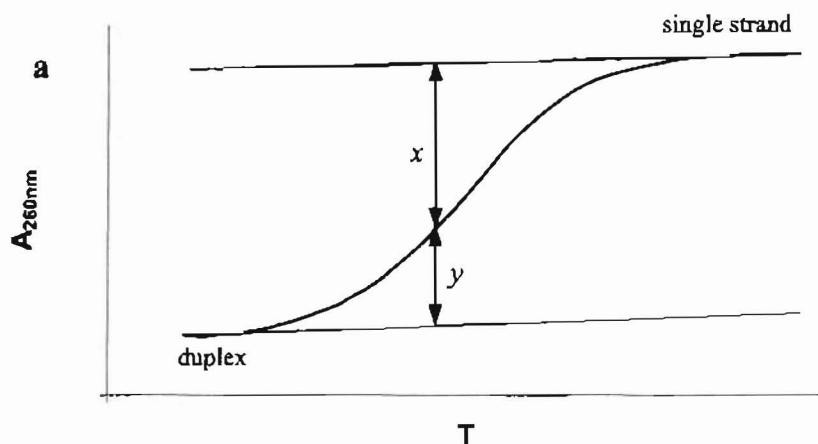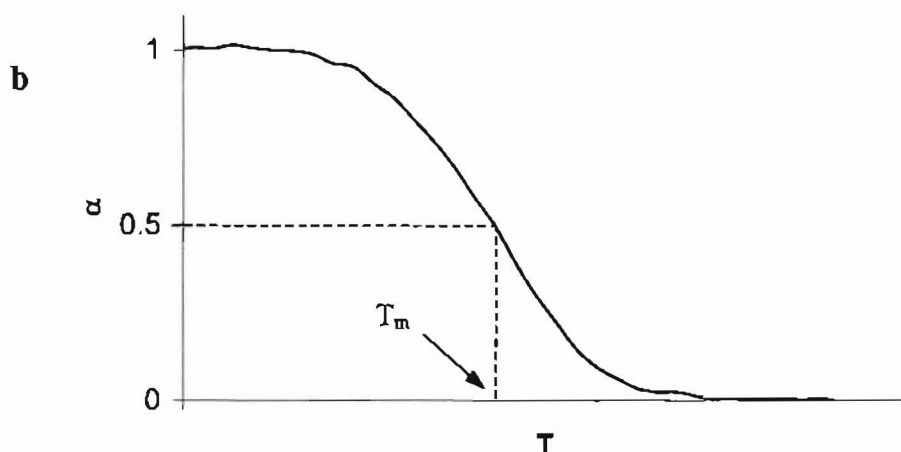
Figure 20: (a) A typical absorbance-vs.-temperature melting curve. where x is the distance from upper base line to curve and y is the distance from curve to lower base line. (b) α plot derived from (a) as described in the text.

For small DNA duplexes melting can be assumed to be an all or nothing process, that is, DNA is either single strand or duplex form and melting occurs in one step. If one assumes that the change in absorbance of duplex with temperature is compensated for by the change for single strand then the fraction of single strands that are in the duplex state at a given temperature can be expressed as $\alpha = x /(x + y)$ and the melting temperature T_m is obtained as the temperature when $\alpha = 0.5$ (Fig. 20b)

Since this transition equilibrium is affected by concentration, the T_m thus obtained has a concentration dependence in accordance with Le Chatlier's principle such that higher concentrations of DNA will require more thermal energy to reach T_m. Consider the equilibrium for two single strands associating to form one duplex molecule:

$$S_1 + S_2 \rightleftharpoons S_1 \bullet S_2$$

The equilibrium constant (K_{eq}) for this transition is given by

$$K_{eq} = \frac{[S_1 \bullet S_2]}{[S_1] * [S_2]} \qquad (i)$$

42

and assuming that S_1 and S_2 are present in equal concentration, then we can express all the concentrations above in terms of the total concentration of single strands in solution (C_T). Thus at a given temperature we have

$$[S_1 \cdot S_2] = \alpha(C_T/2) \qquad \text{(ii)}$$

$$[S_1] = [S_2] = (1 - \alpha)(C_T/2) \qquad \text{(iii)}$$

Substituting (ii) and (iii) into (i) gives

$$K_{eq} = \frac{\alpha(C_T/2)}{[(1-\alpha)C_T/2]*[(1-\alpha)C_T/2]} = \frac{\alpha(C_T/2)}{[(1-\alpha)C_T/2]^2} \qquad \text{(iv)}$$

Taking the melting temperature to be when $\alpha = 0.5$ in the above expression [Eq. (iv)] gives:

$$K_{eq} = \frac{(1/2)(C_T/2)}{[(1/2)C_T/2]^2} = \frac{1}{(1/2)(C_T/2)} = \frac{4}{C_T} \qquad \text{(v)}$$

For any equilibrium, $\Delta G = -RT \ln K_{eq}$ and in the case of the melting transitions then:

$$\Delta G = -RT_m \ln K_{eq}$$

and also $\Delta G = \Delta H - T\Delta S$ such that at the melting equilibrium we have:

$$\Delta G = \Delta H - T_m \Delta S$$

Equating the two expressions of ΔG at the melting temperature gives:

$$-RT_m \ln K_{eq} = \Delta H - T_m \Delta S \qquad \text{(vi)}$$

and substituting Eq. (v) into Eq. (vi) gives:

$$-RT_m \ln (4 / C_T) = \Delta H - T_m \Delta S$$

and rearranging the equation gives:

$$\frac{1}{T_m} = \frac{R}{\Delta H} \ln C_T + \frac{\Delta S - R \ln 4}{\Delta H}$$

and thus a plot of $1/T_m$ vs. ln C_T is a linear plot with slope $\dfrac{R}{\Delta H}$ and intercept

$\dfrac{\Delta S - R \ln 4}{\Delta H}$ (Fig. 21).
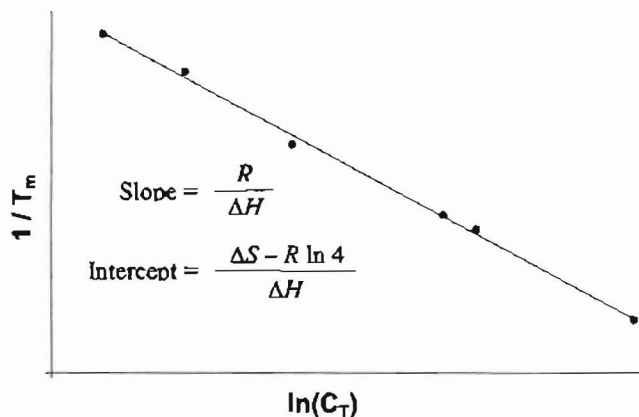
Figure 21: van't Hoff plot for concentration dependence of T_m. C_T total is the concentration of single strands in solution.

Melting Temperatures

Melting temperatures were determined as described above and four experimental T_m's were averaged to determine the T_m for a given duplex at a particular concentration. The α-plots for the melting transition at ~6 μM concentration are shown in Fig. 22 below for comparison.

T_m values calculated at 6 μM duplex concentration are summarized in Table 2 below. The values indicate that all the altered duplexes have decreased stability compared to **1·2** duplex that contains the normal Watson-crick G·C base pairing.
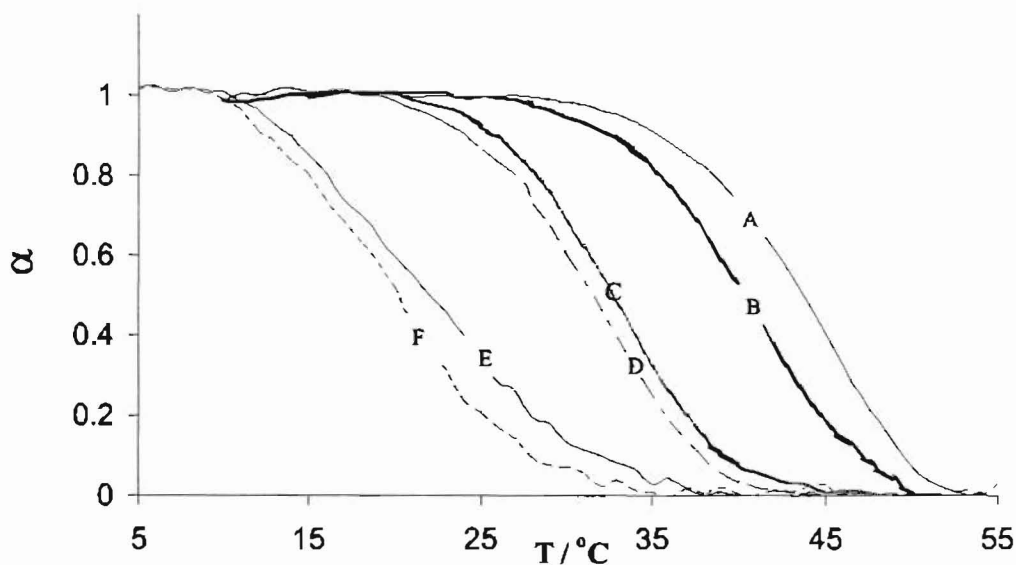
Figure 22: α plots for melting profiles obtained in phosphate buffer (10 mM PO_4^{3-}, 100 mM NaCl, 1 mM EDTA, pH = 6.8-7.2). Temperature ramp: 5 °C - 55 °C in 1 °C steps, 60 s equilibration time at each temperature. A) G•C duplex, (B) ^{6S}G•C, (C) G•T, (D) ^{6S}G•T (E) ^{Me6S}G•C and (F) ^{Me6S}G•T

Table 3: Summary of T_m values for duplexes compared to the duplex with normal Watson-Crick GC base pair.

Duplex	T_m (~6μM) / °C	ΔT_m / °C *
GC	43.8(2)	-
^{6S}GC	40.1(3)	3.7
^{Me6S}GC	28.2(5)	15.6
GT	31.2(2)	12.6
^{6S}GT	30.1(4)	13.7
^{Me6S}GT	24.3(7)	19.5

*compared to duplex (with normal G C base pair)

The value for the G•T mismatch is depressed by 12.6 °C and may indicate the presence of

Wobble base pairing (Fig 23), which affords only 2 hydrogen bonds compared to three in

pairing with C.

45
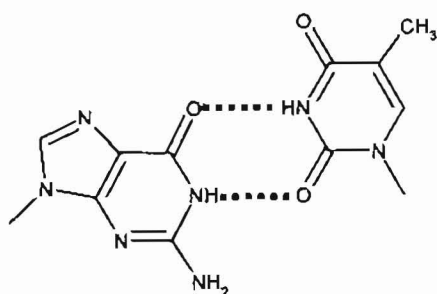
Figure 23: Wobble G•T base pair

Values for duplexes containing ^{6S}G have T_m depressed by 2-3 °C compared to the corresponding values for duplexes containing G. This suggests that unlike what theory may predict, the thermal stabilities for duplexes containing ^{6S}G is comparable to that for the G-containing duplexes. This also strongly suggests that the source of thermal destabilization for the ^{6S}G•T mismatch is similar to that in the G•T mismatch when compared to duplexes with ^{6S}G•C and G•C pairing respectively. In addition, the similarity in the difference between the corresponding duplexes containing ^{6S}G vs. G ($\Delta T_m = 3.7$ °C for G•C/ ^{6S}G•C and 1.1 °C for G•T/ ^{6S}G•T) indicates that the ^{6S}G•T mismatch is not stabilized compared to the G•T mismatch as would have occurred if ^{6S}G was in the thiol form as predicted by theoretical calculations (21) and experiments with isolated ^{6S}G (10). T_m values for duplexes with ^{Me6S}G are depressed by at least 15 °C in both cases, which means that these duplexes are significantly less thermally stable compared to either G or ^{6S}G-containing duplexes. This may indicate that the presence of the S6-methyl introduces hydrophobic interactions within the hydrogen-bonded interior of the double helix. Thus, increased hydrogen bonding distances may be present even in the neighboring bases. Comparing the ^{Me6S}G•C to the ^{Me6S}G•T mismatch, the results suggest that thermal

destabilization is probably due to a similar effect in these two duplexes and is different from thermal destabilization in duplexes containing ^{6S}G. A possibility is that in the case of ^{6S}G, both Watson-Crick and wobble base pairing are present and the observed lower T_m is due only to the increased radius and reduced electronegativity of S. In the case of ^{Me6S}G, presence of a methyl group could prevent Watson-Crick hydrogen bonding interaction (Fig. 24) as was shown to be the case for O6-methyl guanine, where only one H-bond is possible with T (19).
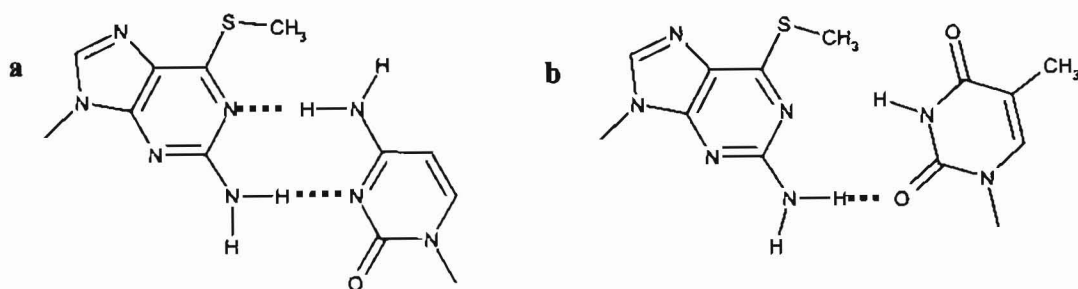
Figure 24: Possible (a) wobble ^{Me6S}G•C and (b) ^{Me6S}G•T interactions in solution, only one H- bond is possible due to the stearic interactions involving methyl group(19)

It is also possible for the Me-group to point away from the opposite base in which case wobble base pairing may be possible with C and a Watson-Crick type interaction with two hydrogen bonds is possible with T. Another factor contributing to the destabilization is that methyl hydrogens are always out of the plane of the DNA base, which results in expansion of the base stacking distances, and this may be the most important contributor to the destabilization in both duplexes.

Van't Hoff thermodynamic parameters

Thermodynamic properties of DNA are affected by three main interactions to give the overall free energy change of the transition from duplex to single strands at elevated temperatures. The free energy change associated with formation of a single base pair is negative due to the formation of hydrogen bonds between the bases (3). Thus for a duplex, one expects a positive free energy change in going from duplex to single strand. The first considerations are that of the DNA internal make up, which is made up of hydrogen bonding and base stacking interactions. Since the G•C base pair is held together by three hydrogen bonds and A•T by only two, duplexes with higher G•C proportion will have a higher free energy change. Similarly, duplexes in which the hydrogen bonding interactions are disrupted would have a lower ΔG for melting transitions. The final consideration of the DNA molecule is the phosphate interactions. Phosphates are moderate acids and at physiological and experimental pH's they are ionized giving a net repulsion within the DNA backbone (17). This repulsion is counteracted by the presence of cations, mainly K^+ in cells and Na^+ in the experimental buffer used. Thus the separation of the phosphates in the DNA structure as well as salt concentration will affect the overall free energy change. The second consideration is that of the solvent, which consists of solvation of the DNA strands as well as salt interactions as mentioned above. In our case solvation of DNA may play an important role in affecting ΔG since O6 in case of G and S6 in the case of [6S]G and MeS6 for [Me6S]G are solvated considerably differently by water molecules in solution as predicted by theoretical calculations for O6 vs. S6 (20).

A summary of the van't Hoff thermodynamic parameters for the duplexes is given below in Table 4 with a comparison to the G•C duplex.

Table 4: Summary of van't Hoff Thermodynamic parameters

Duplex	ΔH_{vH}° kcal/mol[a]	ΔS_{vH}° cal/mol	$\Delta G_{vH}^{\circ}{}_{25}$ kcal/mol	$\Delta\Delta H_{vH}^{\circ}$ kcal/mol[b]	$\Delta\Delta S_{vH}^{\circ}$ cal/mol[b]	$\Delta\Delta G_{vH}^{\circ}{}_{25}$ kcal/mol[b]
G C	92(2)	267(5)	12.5(3)			
[6S]G C	132(2)	394(9)	14.3(4)	-40	-127	-1.8
[Me6S]G C	62(3)	253(5)	-13.4(5)	30	14	25.9
G T	120(2)	365(8)	11.3(3)	-28	-98	1.2
[6S]G T	58(2)	165(5)	8.9(4)	34	102	3.6
[Me6S]G T	68(7)	270(9)	-12.5(8)	24	-3	25.0

[a] values are per mol of duplex melting. Values were obtained using concentration dependence of melting equilibrium.

[b] $\Delta\Delta(H_{vH}^{\circ}, S_{vH}^{\circ}, G_{vH}^{\circ})_{duplex} = \Delta(H_{vH}^{\circ}, S_{vH}^{\circ}, G_{vH}^{\circ})_{duplex} - \Delta(H_{vH}^{\circ}, S_{vH}^{\circ}, G_{vH}^{\circ})_{G-C duplex}$

Results show that at 25 °C the ΔG_{vH} for the transition is highest for [6S]G•C duplex followed by G•C duplex and is negative for the duplexes containing [Me6S]G. For the [6S]G•C we see that enthalpy of transition is higher compared to G•C and the lower melting temperature of the former is due to larger entropy of transition, which dominates ΔG above 40 °C. This may suggest that the [6S]G•C base pair may in fact have similar thermodynamic stability compared to G•C at physiological temperature, contrary to predictions from theoretical considerations (21). The higher enthalpy of melting may result from the S6 in [6S]G being less efficiently solvated in the single strand compared to O6 in G and possibly increased base stacking energy in the [6S]G•C duplex. For the G•T and [6S]G•T mismatches, ΔG is below that of the corresponding duplexes showing that the

mismatches are destabilized at 25 °C. Inspecting the ΔH and ΔS however gives opposite trends which may suggest that the source of destabilization may be different in these two duplexes, for example solvation may play a larger role in one but not in the other. Also judging from the general trend for the duplexes it appears that the values for G•T mismatch may be off possibly due to error in concentration determination as the extinction coefficient may suggest. ΔG values for duplexes containing ^{Me6S}G are similar and negative at 25 °C, which suggests that these duplexes prefer to be in the single strand state at this temperature. For both ^{Me6S}G•C and ^{Me6S}G•T, ΔH is much lower than that of either G•C or ^{6S}G•C whereas ΔS is comparable to that of the G•C duplex. This supports the fact that duplexes containing ^{Me6S}G are thermodynamically destabilized significantly compared to unmodified duplexes due to the presence of a methyl group, which may disrupt both base stacking interactions between neighboring bases and hydrogen bonding interactions between base pairs (19, 23). In addition distortion of the DNA duplex backbone may give rise to unfavorable phosphate interactions, which further destabilize these duplexes.

In summary, the results obtained here suggest that duplexes containing ^{6S}G may be similar in structure and stability compared to duplexes with unmodified G whereas duplexes containing ^{Me6S}G are considerably destabilized.

Significance of Results

The results obtained here do not give a clear picture of what might be the source of destabilization of duplexes containing the modified bases ^{6S}G and ^{Me6S}G since one

cannot resolve contributions of solvent, base-stacking, and electrostatic interactions. This study, however, suggests what might be going on at the molecular level for the cytotoxicity associated with administration of ^{6S}G or its prodrugs. The results are consistent with the observation that incorporation of ^{6S}G does not introduce significant destabilization of the DNA duplex (20). In addition the fact that destabilization is due to a higher entropy of melting may be consistent with the fact that theoretical calculations predict a significant difference in the first hydration shell of S6 in ^{6S}G compared to O6 in G (20). In effect, this suggests that incorporated ^{6S}G may act via alteration of DNA-protein interactions (2, 11, 22) or that miscoding of T opposite ^{6S}G may be an important step rather than direct destabilization of DNA duplex (19).

The destabilization of duplexes containing ^{Me6S}G on the other hand is significant compared to those containing unmodified G or ^{6S}G. This may mean that duplexes containing ^{Me6S}G are destabilized enough to directly affect normal nucleic acid functions, which may mean that methylation is a key step in the biological action of ^{6S}G. In addition, the similarity between ^{Me6S}G•C and ^{Me6S}G•T suggests that miscoding of T opposite ^{Me6S}G may not be a required step for the biochemical effect to occur. This may be consistent with the discovery that hMutSα, the human mismatch binding protein dimer binds to ^{Me6S}G•C base pair when in sequence with a C 5' to the modified guanine (5' –C^{Me6S}G – 3') (23). And since CpG sequence is associated with gene silencing and transcription, binding of hMutSα to 5'-Cp^{Me6S}G may affect key gene functions and this may trigger events leading to cell death. Thus sequence dependence, which is not considered here, may play an important role in the effect of ^{6S}G and ^{Me6S}G in cells and as such may be an important area of expansion for this project.

Conclusions:

To understand the effect of ^{6S}G on stability of DNA duplexes, thermodynamic parameters were obtained for a series oligonucleotides containing ^{6S}G-C, ^{Me6S}G·C and G·C base pairs as well as the corresponding G·T mismatches. Results show that the presence of S6 in place of O6 in ^{6S}G leads to a small destabilization of the DNA duplex. On the other hand, incorporation of ^{Me6S}G leads to more significant destabilization of DNA duplex. Although it is difficult to resolve the various interactions that give rise to observed free energy change for the melting transitions, general ideas can be drawn form the results of this project. The destabilization of duplex by incorporated ^{6S}G is dominated by entropy of melting rather than the enthalpy, which may suggest that base stacking and solvation effects play a larger role than disruption of hydrogen bonding. The enthalpy and entropy of transition for duplexes containing ^{Me6S}G is very similar, which suggests that destabilization in these duplexes may be due to a significant disruption of DNA structure, possibly including hydrogen bonding, base stacking and phosphate interactions of the DNA backbone.

Future Work:

Several investigations need to be carried out before results reported here are used to make conclusions on the role of ^{6S}G in the cytotoxicity pathway for anti-tumor agents. It is clear that resolving the different interactions that give rise to observed stability for DNA duplexes using melting temperature alone is not possible, hence combining this research with studies such as NMR on the same duplexes is necessary. Also, since the thermodynamic parameters obtained here are model dependent, it is necessary to obtain data on these duplexes from an independent experiment. Differential scanning calorimetry (DSC) is one possibility that is being considered and has the advantage that it gives model-independent data. A combination of these studies may give a clearer understanding of the changes in structure of DNA containing the altered bases ^{6S}G and ^{Me6S}G.

References:

1. Ali, S.; Lebwohl, M. Treatment of Psoriasis. Part 2. Systemic therapies. *J. Am. Acad. Dermatol.*, **2001**, *45*, 649-661

2. Aubrecht, J.; Goad, M. E. P.; Schiestl, R. H. Tissue specific toxicities of the anticancer drug 6-thioguanine is dependent on the hprt status in transgenic mice. *J. Pharm. Expt. Ther.* **1987**, *282*, 1102-1108

3. Breslauer, K. J. Extracting thermodynamic data from equilibrium melting curves for oligonucleotide order-disorder transitions. *Methods in Enzymology*, **1987**, *259*, 221-242

4. Bugg, C. E.; Thewalt, U. Crystal and molecular structure of 6-thioguanine. *J. Am. Chem. Soc.* **1970**, *92*, 7441-7445

5. Christopherson, M. S.; Broom, A. D. Synthesis of oligonucleotides containing 2'-deoxy-6-thioguanosine at a predetermined site. *Nucleic Acids Research*, **1991**, *19*, 5719-5724

6. Coleman, R. S.; Arthur, J. C.; McCary, J. L. 6-Thio-2'-deoxyinosine: synthesis, incorporation and evaluation as a postsynthetically modifiable base in oligonucleotides *Tetrahedron*, **1997**, *53*, 11191-11202

7. Dubnisky, M. C.; Hassard, P. V.; Seidman, E. G.; Kam, L. Y.; Abreu, M. T.; Targan, S. R.; Vasiliauskas, E. A. An open pilot study using thioguanine as a therapeutic alternative in Crohn's disease patients resistant to 6- mercaptopurine therapy. *Inflamm. Bowel Dis.*, **2001**, *7*, 181-189

8. Elion, G. B. The purine path to chemotherapy. *Science*, **1989**, *244*, 41-47

9. Griswold, B. L.; Humoller, F. L.; McIntyre, A. R. Inorganic phosphates and phosphate esters in tissue extracts. *Analytical Chemistry*, **1951**, *23*, 192-194

10. Kasende, E. O. Infrared spectra of 6-thioguanine tautomers. An experimental and theoretical approach. *Spectrochimica Acta Part A*, **2001**, *(proof)*

11. Krynetskaia, N. F.; Feng, J. Y.; Krynetski, E. Y.; Garcia, J. V.; Panetta, J. C.; Anderson, K. S.; Evans, W. E. Deoxythioguanosine triphosphate impairs HIV replication: A new mechanism for an old drug. *FASEB*, **2001**, *15*, 1902-1908

12. Le Page, G. A. basic biochemical effects and mechanism of action of 6-thioguanine *Cancer Research*, **1963**, *23*, 1202-1206

13. Marathias, V. M.; Sawicki, M. J.; Bolton, P. H. 6-Thioguanine alters the structure and stability of duplex DNA and inhibits quadraplex formation. *Nucleic Acids Research*, **1999**, *27*, 2860-2867

14. Milton, J.; Connolly, B. A.; Nikiforov, T. T.; Cosstick, R. Site-specific disulfide bridges in oligoribonucleotide duplexes containing 6-mercaptopurine and 4-thiothymine bases. *J. Chem. Soc., Chem. Commun.*, **1993**, 779-780

15. Pike, M. G.; Franklin, C. L.; Mays, D. C.; Lipsky, J. J.; Lowry, P. W.; Sandborn, W. J. Improved methods for determining the concentration of 6-thioguanine nucleotides and 6-methylmercaptopurine nucleotides in blood. *J. Chromatogr. B*, **2001**, *757*, 1-9

16. Rao, T. S.; Durland, R. H.; Seth, D. M.; Myrick, M. A.; Bodepuli, V.; Revankar, G. R. Incorporation of 2'-deoxy-6-thioguanosine into G-rich oligoribonucleotides inhibits G-tetrad formation and facilitates triplex formation *Biochemistry*, **1995**, *34*, 765-772

17. Rychlik, W.; Rhoads, R. E. A computer program for choosing optimal oligonucleotides for filter hybridization, sequencing and in vitro amplification of DNA. *Nucl. Acids. Res.* **1989**, *17*, 8543-8551

18. Serra, M. J.; Turner, D. H. Predicting thermodynamic properties of RNA. *Methods in Enzymology*, **1987**, *259*, 242-261

19. Spratt, T. E.; Levy, D. E. Structure of the hydrogen bonding complex of O6-methylguanine with cytosine and thymine during DNA replication. *Nucleic Acids Research*, **1997**, *25*, 3354-3361

20. Šponer, J.; Leszczynski, J.; Hobza, P. Thioguanine and thiouracil: hydrogen bonding and stacking properties. *J. Phys. Chem. A.*, **1997**, *101*, 9489-9495

21. Stewart, M. J.; Leszczynski, J.; Rubin, Y. V.; Blagoi, Y. P. Tautomerism of thioguanine: From gas phase to DNA. *J. Phys. Chem.*, **1997**, *101*, 4753-4760

22. Tendian, S. W.; Parker, W. B. Interaction of deoxyguanosine nucleotide analogs with human telomerase. *J. Pharm. Expt. Ther.* **2000**, *57*, 695-699

23. Waters, T. R.; Swann, P. F. Cytotoxic mechanism of 6-thioguanine: hMutSa, the human mismatch binding heterodimer, binds to DNA containing S6-methylthioguanine. *Biochemistry*, **1997**, *36*, 2501-2506

24. Wijnholds, J.; Mol, C. A. A. M.; van Deemter, L.; de Haas, M.; Scheffer, G. L.; Baas, F.; Beijnen, J. H.; Scheper, R. J.; Hatse, S.; De Clercq, E.; Balzarini, J.; Borst, P. Multidrug-resistance protein 5 is a multispecific organic anion transporter able to transport nucleotide analogs. *PNAS,* **2000**, *97*, 7476-7481